FWI time-lapse monitoring of CO2 injection using VSP at CaMI FRS: a feasibility study

Ninoska Amundaray, Kris Innanen, Marie Macquet and Don C. Lawton

ABSTRACT

Full waveform inversion (FWI) holds a strong potential for reservoir monitoring due to its proven capabilities to determine high-resolution subsurface models. An expanding branch of reservoir monitoring, seismic time-lapse, aims to image variations in the elastic properties of selected formations due to carbon dioxide (CO_2) storage. Several datasets and technologies are being assessed to verify secured containment of the gas, among others, vertical seismic profiles (VSP). Previous investigations for the Containment and Monitoring Institute Field Research Station (CaMI FRS) suggest changes in the bulk and shear moduli in a shallow reservoir for a CO_2 injection program of a maximum 1664 tons. In this paper, we modeled two sensor dispositions with two different source arrangements of VSP, to evaluate the performance of an FWI algorithm at this geological setting. A multiscale approach with nine frequency bands (4-8 Hz, 4-12 Hz, 4-16 Hz, 4-20 Hz, 4-24 Hz, 4-28 Hz, 4-32 Hz, 4-36 Hz and 4-40 Hz) was utilized to evaluate three stages of gas injection from a baseline to a five-year period. Inverted models converged towards the true solution suggested from previous projections. Time-lapse results reproduce a reduction of P-wave velocity for near and far offsets, registering a maximum 17% decrease at reservoir levels. At these depths, model resolution does not appear to be particularly influenced by the amount and distribution of receivers, as much as it is controlled by number of modeled sources.

INTRODUCTION

Seismic time-lapse reservoir monitoring is the process of acquiring and analyzing multiple seismic surveys throughout a regular period of time, in order to image fluid-flow effects in a producing reservoir (Lumley, 2001). These effects correspond with variations of pressure, saturation and temperature during production stage in hydrocarbon exploitation and a fluid injection phase in carbon capture and storage projects, and in a lesser degree after reservoir depletion. Time-lapse seismic datasets are expected to record reservoir changes through a combination of variations in amplitude and travel time, which are intrinsically associated to the elastic properties of the rocks.

Imaging techniques for seismic time-lapse includes regular seismic processing and inversion procedures. In the last years, a method that has started to be increasing applied in the latter case to determine high-resolution subsurface models is full waveform inversion (FWI) in both, marine and land environments. Applications of FWI have been able to capture features of subsurface properties that were not resolved by conventional velocity analysis (Smithyman et al., 2015; Pan et al., 2017), making FWI particularly suitable for reservoir monitoring purposes.

Recent studies of FWI using vertical seismic profiles (VSP) demonstrate additional benefits to invert for seismic time-lapse images. One of them, it is a fixed seismic acquisition, which ensures that seismic rays travelling an area are recorded with a similar

direction, minimizing effects caused by variations in acquisition and providing datasets that truthfully represent changes in the reservoir properties. Alongside this, the deployment of receivers buried in depth and secured on the walls of a borehole in VSP, protect them against most of the surface-related noise sources enabling surveys with high signal-to-noise ratio (Cova et al., 2018).

Nowadays, there is an expanding branch of reservoir monitoring associated with carbon dioxide (CO_2) storage in the subsurface within geological formations that meet certain criteria. This method is expected to contribute in the reduction of greenhouse gas emissions into the atmosphere that many countries pledged, and hence, several monitoring datasets and techniques are being used to assess its effectiveness on selected reservoirs. Anticipated results of this method include, but are not limited to, the identification of changes in the elastic properties of rocks in reservoir intervals due to the addition of CO_2 and the detection of potential hazards.

The Containment and Monitoring Institute (CaMI) developed the Field Research Station (FRS) in collaboration with the University of Calgary to facilitate and accelerate research and development leading to improved understandings and technologies for geological containment and secure storage of CO_2 (Macquet et al., 2019). A permanent VSP experiment has been deployed at the site and regular acquisitions of this type of seismic survey have been recorded in last years. Utilizing model projections of the effects of CO_2 at the FRS, we investigate the feasibility of an acoustic FWI to resolve and monitor the gas injection after one and five years, in a shallow reservoir.

THE CONTAINMENT AND MONITORING INSTITUTE FIELD RESEARCH STATION

Location and geology setting

The FRS is located in southern Alberta, approximately 200 km southeast of Calgary, near the town of Brooks in Newell County. At this site, it hosts a multidisciplinary project which primarily objective is understanding emerging technologies in geophysics and monitoring approaches for carbon capture and storage and its applicability within Canada in a shallow subsurface interval where a small amount of CO_2 is being injected.

The regional geology of the Southern Alberta Plains where the FRS is located, it is described as a succession of strata of Quaternary glacial tills, a section of interbedded coal seams, sandstone, siltstone and shale of Cretaceous age and a Paleozoic succession of carbonate that overlie unconformably the Precambrian basement (Wright et al. 1994). The current injection target at the FRS is a fine-to-medium-grained basal sandstone in the Foremost Formation (Fm.) which was deposited in a coastal to shallow-marine environment within the Belly River Group (Hamblin and Abrahamson, 1996). At this location, the Basal Belly River Sandstone (BBRS) represents a thin 6 m interval between 295.65 and 301.65 m overlain by interbedded mudstones, fine-grained sandstones and coal layers which provide the seal for the CO_2.

Permanent VSP experiment

At the FRS, there is a permanent arrangement of 3C downhole geophones cemented outside of the casing in the observation well 2, located at 20 m SW from the injection well. These sensors are surveying part of the interval of the Foremost Fm. and the upper section of the Leak Park Fm. with a spacing of 5 m between 190 to 305 m depth, as illustrated in Figure 1(a). Multiple walk-away and walk-around VSP datasets centered on this well have been acquired throughout the last years with an approximated source point distance of 60 m. The repeatability of the surveys is intended to monitor, analyze and model changes in the BBRS due to the CO_2 injection.

2018 3D VSP experiment

This was a one time experiment carried out at CaMI FRS in September 2018, where CREWES acquired a multi-azimuth walk-away three-component VSP dataset centered on the observation well 2 for applications of FWI and modeling studies (Hall et al., 2018). The acquisition design consisted in the deployment of thirteen lines of shot points centered on the well with 10 m spacing for four of them and 60 m spacing for the rest using an Inova Univib source running a linear 1-150 Hz sweep. During this time, the receiver disposition was a string of 3C VectorSeis geophones in the same well with a 1 m spacing, from the surface to 324 m depth as shown in Figure 1(b).

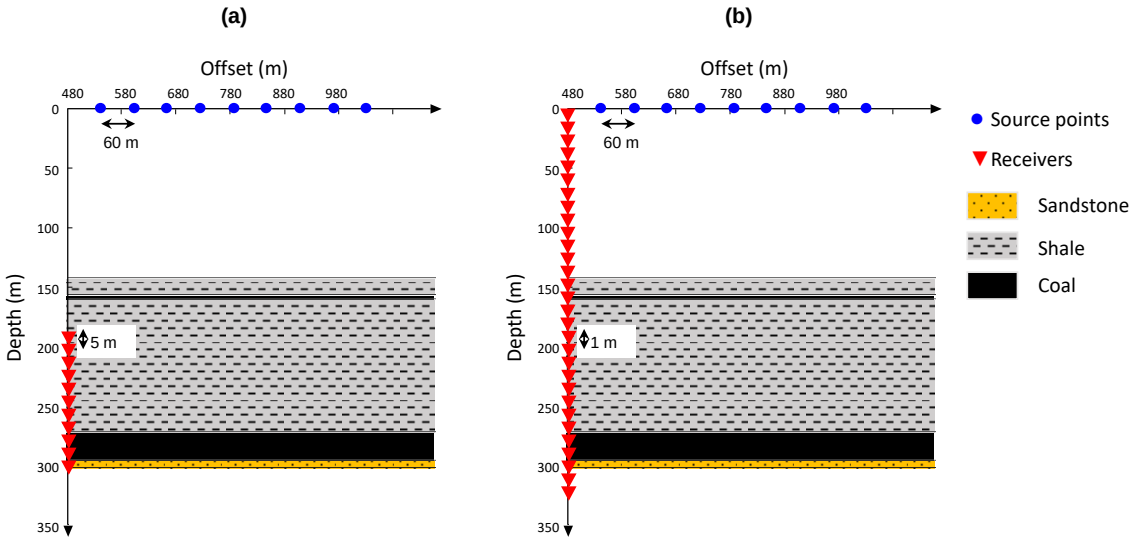

FIG. 1. Schematic of the VSP configurations and the geology of the Belly River Group at CaMI FRS for (a) the permanent VSP experiment and (b) the 2018 VSP experiment. Red triangles represent the arrangement of receivers deployed on the observation well 2 between 190 to 305 m every 5 m in the permanent experiment, and between 0 to 324 m every 1 m in the 2018 experiment. Blue dots represent the source points centered on the well every 60 m within 1 km line.

MODELING THE CO2 INJECTION

Pressure and saturation effects

Macquet et al. (2019) examined the behaviour of the elastic parameters in the BBRS at the FRS produced by an injection program of a maximum 1664 tons of CO_2 for an interval of five years and period of post-closure. The simulation accounted for variations of gas

saturation from 0 to 0.5, fluid and reservoir temperatures and a range of pore pressure between 2.95 to 5.75 MPa using a simple homogenous model with average petrophysical parameters. Results suggested that changes in carbon dioxide saturation will modify the density of the fluid in the reservoir. Whereas a change in the pressure will induce variations in the density and bulk modulus of the CO_2, but more importantly, it will lead a change in the bulk and shear moduli of the dry rock.

After five years of CO_2 injection and the combination of the parameters stated above, a reduction in P-wave velocity of 32% was estimated for the BBRS. The diminution of the velocity is expected to be centered on the injection well reaching initially a maximum diameter of about 40 m and a further expansion up to 200 m after one year and five years of injection, respectively. No upward migration of CO_2 was predicted during this simulation, however a small downward migration of carbon dioxide below the injection zone was calculated due to the permeability derived for modeling.

Time-lapse modeling using FWI

In this issue, Amundaray and Innanen (2020), described in detail how to model VSP acquisitions in Matlab and the acoustic FWI algorithm used in this study. Utilizing the module to simulate seismic experiments, the permanent and the 2018 sensor configurations that have been deployed to record VSP data at CaMI FRS, were reproduced. Two different source arrangements were modeled to test the performance of the algorithm at this geological setting and the effect of source detriment in the inverted model. For source spacing, we kept an equal distance of 60 m and 142 m between shot points, which were modeled with 25 Hz minimum phase wavelet that was chosen based on the frequency spectrum of the real dataset at the FRS.

Three plausible true velocity models for the study area were constructed by Macquet et al. (2019) using the well-log data and the predicted variation of P-wave velocity due to pressure and saturation effects of CO_2 A grid cell size of 5 x 5 m was defined in the horizontal and vertical scale, with a maximum horizontal distance of 1000 m and 500 m in depth for all models.

The true velocity models for CaMI FRS were built from well-log data and for this reason they are very fine-detailed. Nevertheless, applications of FWI are dependent of wavelet parameters as frequency content and sample rate, which are used to model the waveforms that sample a medium and later, are recorded as observed and/or synthetic data. Hence, the medium frequency wavelet utilized in this investigation has a limited and smaller level of resolution if it is compared with the original models obtained from well-logs. In order to keep balance between the earth models at the FRS and the seismic resolution, we smoothed all well-log derived velocity models to some extent and converted them into our adapted version of true models. All results present in this report were estimated from the adapted models; therefore, they will refer as true models.

Figure 2 shows in detail the differences between the P-wave velocity models derived from well-logs and our adapted smoothed versions in a profile view for the baseline model and two stages of CO_2 injection. Although velocity trends are preserved, noticeable spikes

and fine features are loss once the model is smoothed. A full view of our true models is presented in Figure 3.

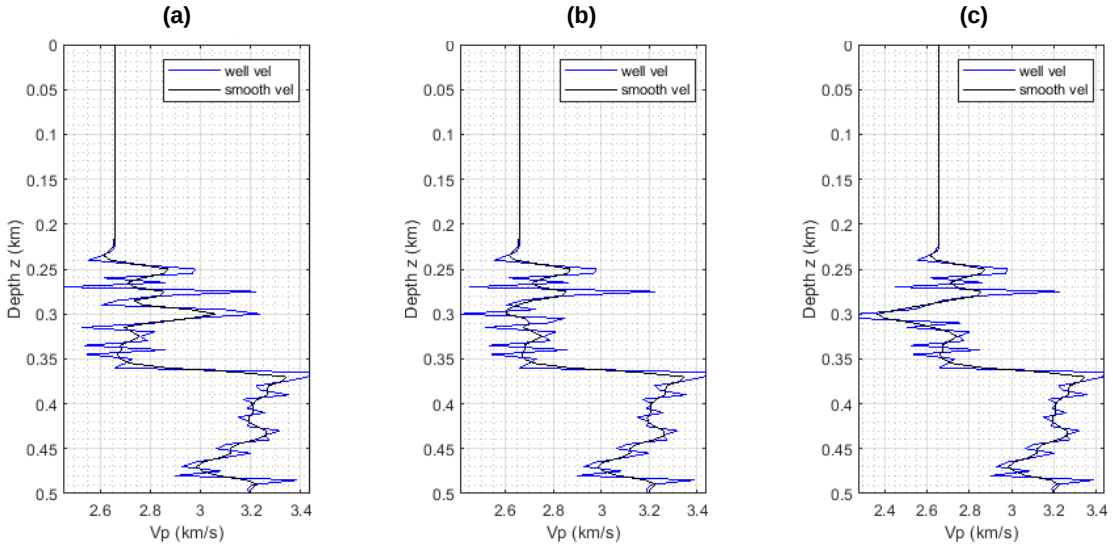

FIG. 2. Profile comparison between the P-wave velocity derived from well-logs and the smoothed velocity adaptation considered in this investigation for modeling a (a) baseline, (b) one year of CO_2 injection and (c) five years of CO_2 injection.

Two profile locations were defined at 40 m and 190 m distance from the receiver arrangement to evaluate the inversion updates in detail at near and far offsets, as indicated in Figure 3(b). These locations also resemble the estimated limits of the effects of CO_2 injection at the BBRS in the P-wave velocity module.

To simulate time-lapse monitoring, we created three observed datasets using the true models for a prior stage before any injection and two stages corresponding to one and five years of CO_2 injection, as has been proposed for the site. We inverted models for each stage using a multiscale approach with nine expanding frequency bands from [4 Hz, 8 Hz] to [4 Hz, 12 Hz], [4 Hz, 16 Hz], [4 Hz, 20 Hz], [4 Hz, 24 Hz], [4 Hz, 28 Hz], [4 Hz, 32 Hz], [4 Hz, 36 Hz] and [4 Hz, 40 Hz]. A maximum of ten iterations per frequency band was allowed and the starting velocity model for the three modeled stages was a smooth version of the true baseline.

Figure 4 displays the inverted models for three frequency bands throughout the different modeled stages using the permanent VSP configuration deployed at the CaMI site. While, Figure 5 illustrates the inversion results for equivalent frequency bands and stages but modeling the 2018 VSP experiment. In both figures, columns represent the same timeframe, whereas rows showcase a quick comparison of the resolved features in the models using the exact frequency content.

A more detailed view of the inversion results is presented in Figures 6 and 7. The profile shows the evolution of model updates from the initial to the final inverted model and the true velocity at the selected locations. Although, intervals of over and underestimation are noticeable, the inversion converged towards the true P-wave velocity values. Most

importantly, the general trends at reservoir depths were recovered for the modeled stages. Once again, column diagrams represent the same timeframe, while row diagrams illustrate the updates through time at each profile location.

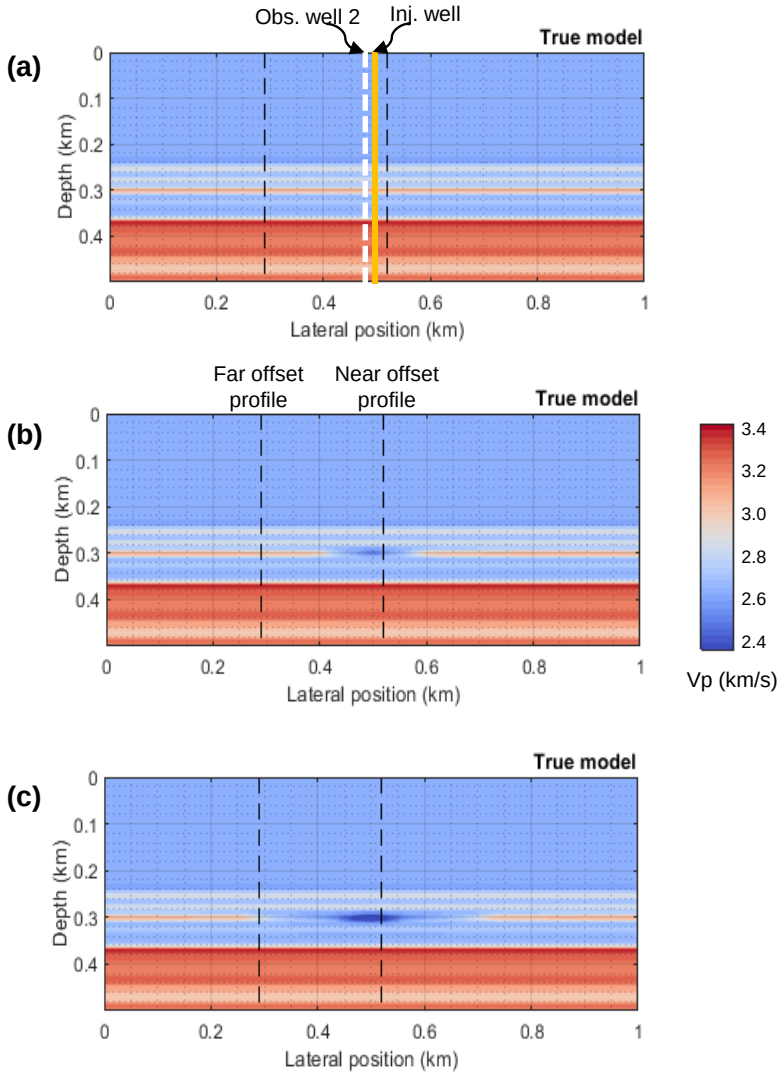

FIG. 3. True P-wave velocity models for the FRS at (a) baseline stage, (b) after one year of CO_2 injection and (c) after five years of CO_2 injection. Locations of the observation well 2 and the injection well are highlighted in the top diagram with a white dashed line and a yellow line, respectively. Profiles locations are overlain in all models with dashed black lines.

As mentioned, a sparse source distribution was tested to evaluate the algorithm performance for the same subsurface model. For this case, the only variation made was source spacing, which was about 142 m. Nonetheless, the receiver dispositions, models, multiscale approach and profile locations were kept consistent. Figures 8 and 10 show results using the permanent sensors arrangement at the FRS, whereas Figures 9 and 11 display results for a sensor distribution similar to the 2018 VSP acquisition.

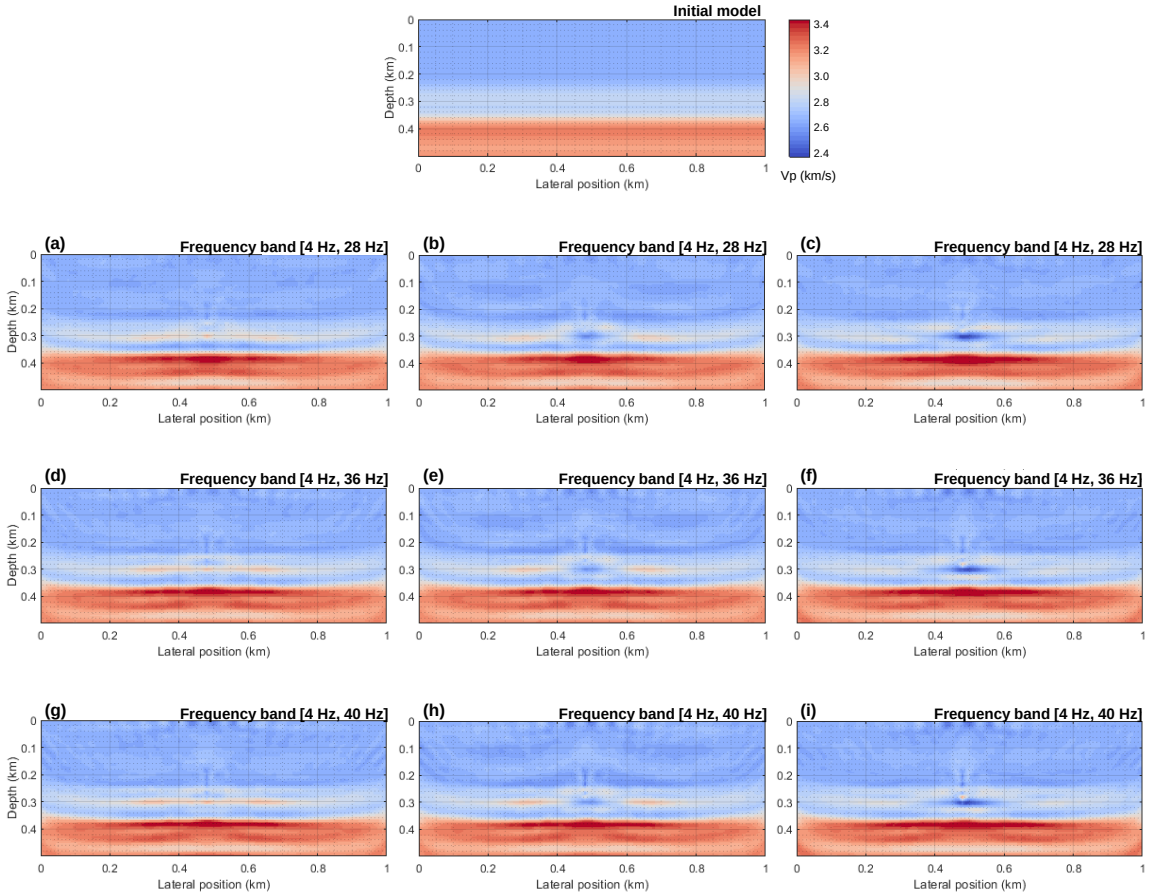

FIG. 4. Inverted models utilizing the permanent VSP experiment design with sensors deployed between 190 to 305 m and a source distribution spaced every 60 m for three different frequency bands at three different stages. Graphs (a), (d) and (g) represent the inverted baseline models, whereas (b), (e) and (h) represent the inverted models after one year of CO_2 injection; and (c), (f) and (i) represent the inverted models after five years of CO_2 injection.

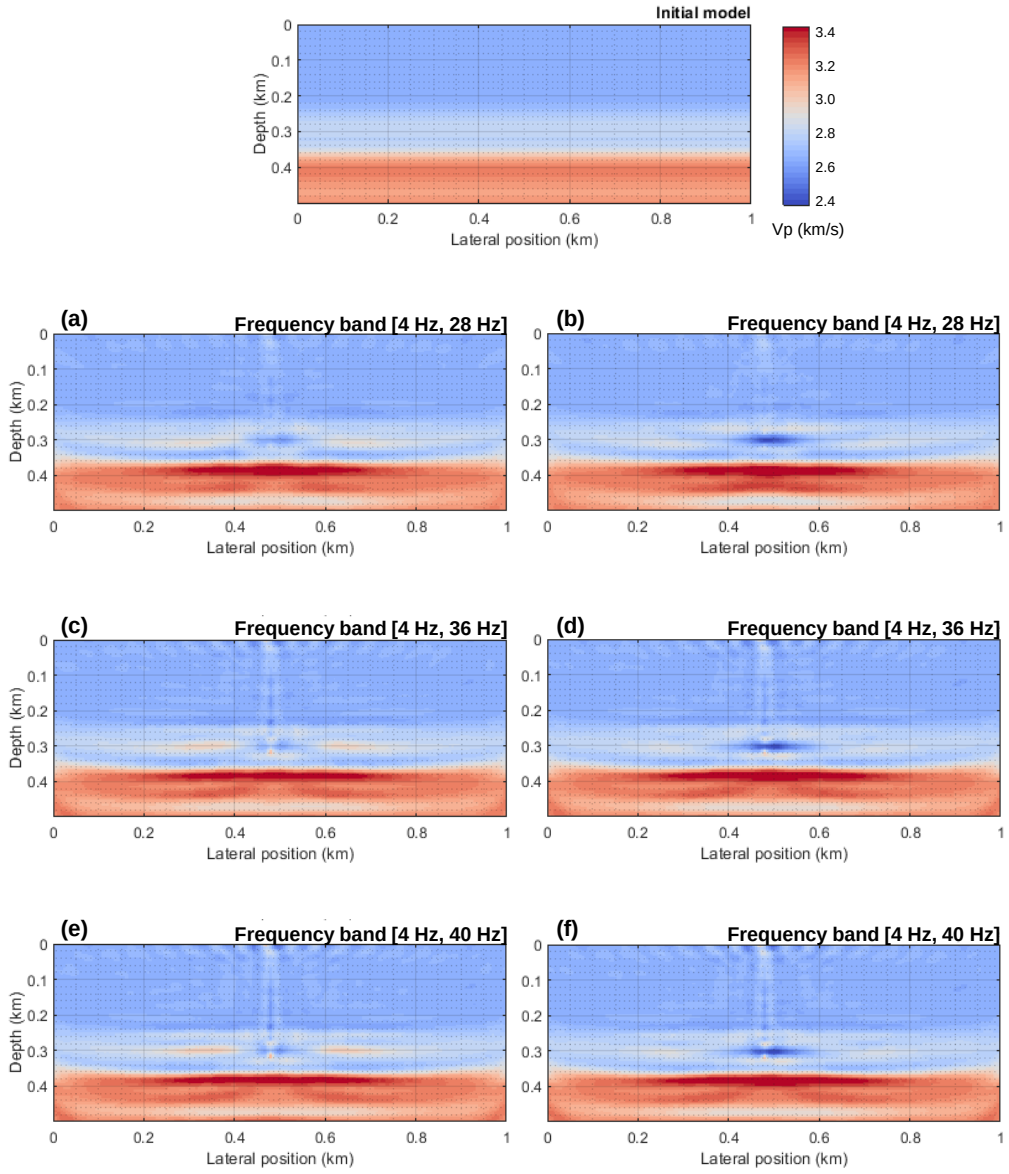

FIG. 5. Inverted models utilizing the 2018 VSP experiment design with sensors deployed between 0 to 324 m and a source distribution spaced every 60 m for three different frequency bands at three different stages. Graphs (a), (c) and (e) correspond to the inverted models after one year of CO_2 injection, while (b), (d) and (f) correspond to the inverted models after five years of CO_2 injection.

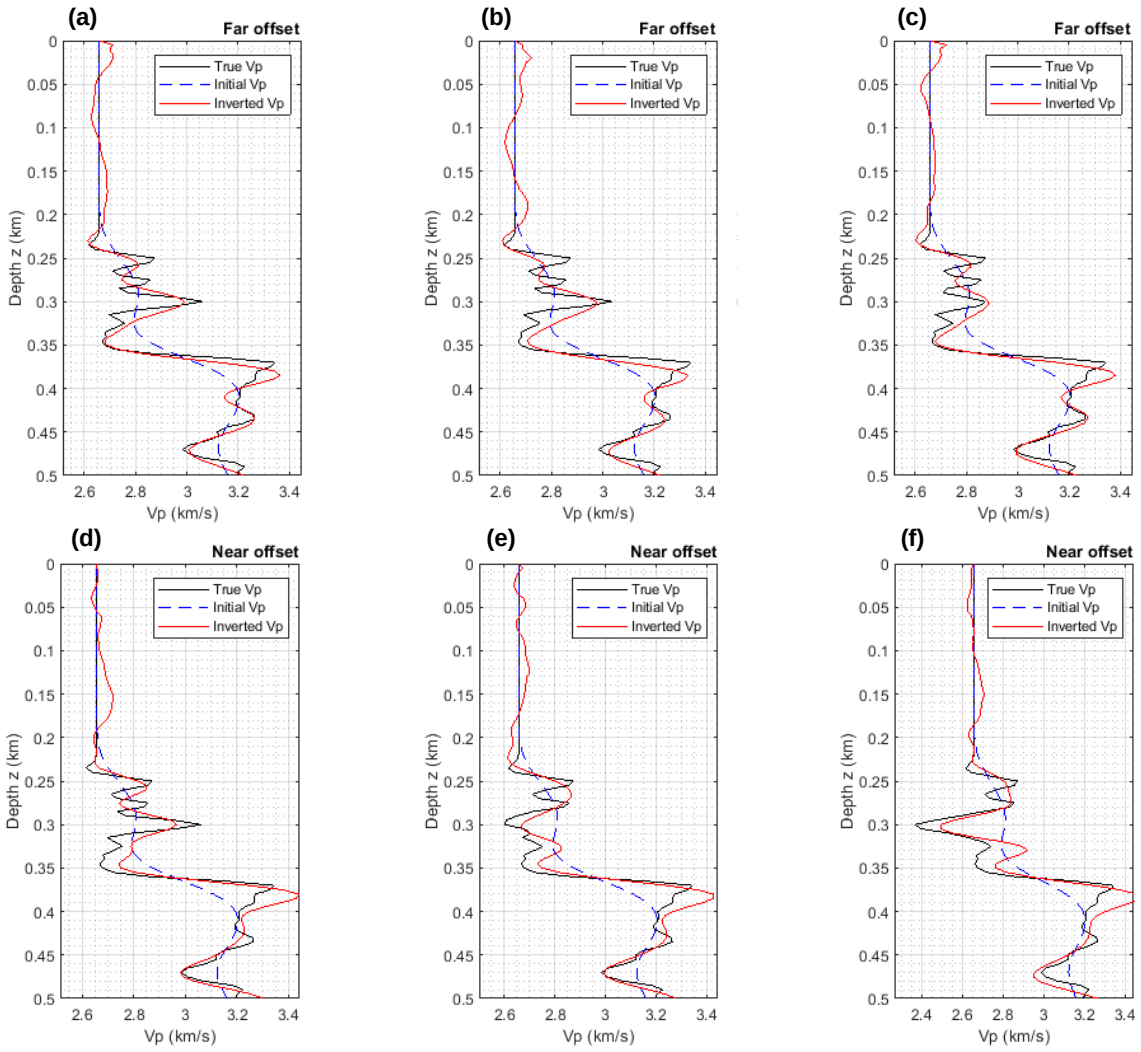

FIG. 6. Profile views of the true, initial and inverted P-wave velocity for far and near offsets consistent with the permanent VSP experiment for three different stages. Graphs (a) and (d) represent the baseline stage, while (b) and (e) represent the effects of one year of CO_2 injection; and (c) and (d) represent the effects of five years of CO_2 injection.

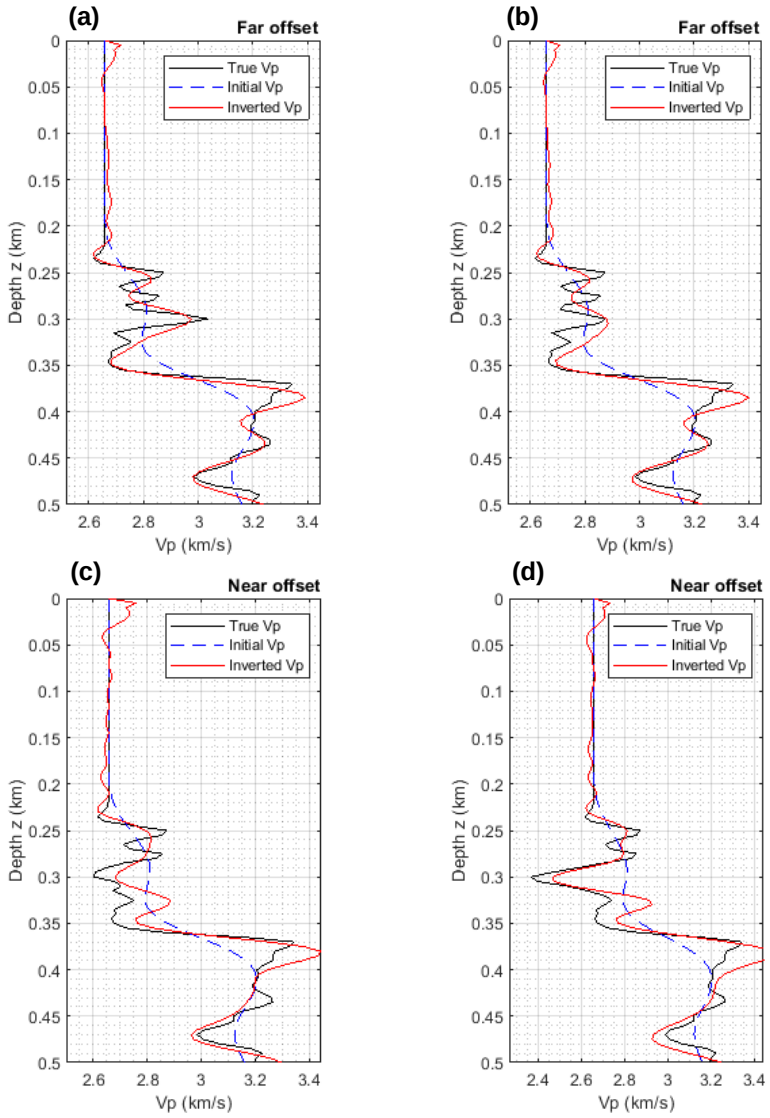

FIG. 7. Profile views of the true, initial and inverted P-wave velocity for far and near offsets consistent with the 2018 VSP experiment for three different stages. Graphs (a) and (c) represent the effects of one year of CO_2 injection; while (b) and (d) represent the effects of five years of CO_2 injection.

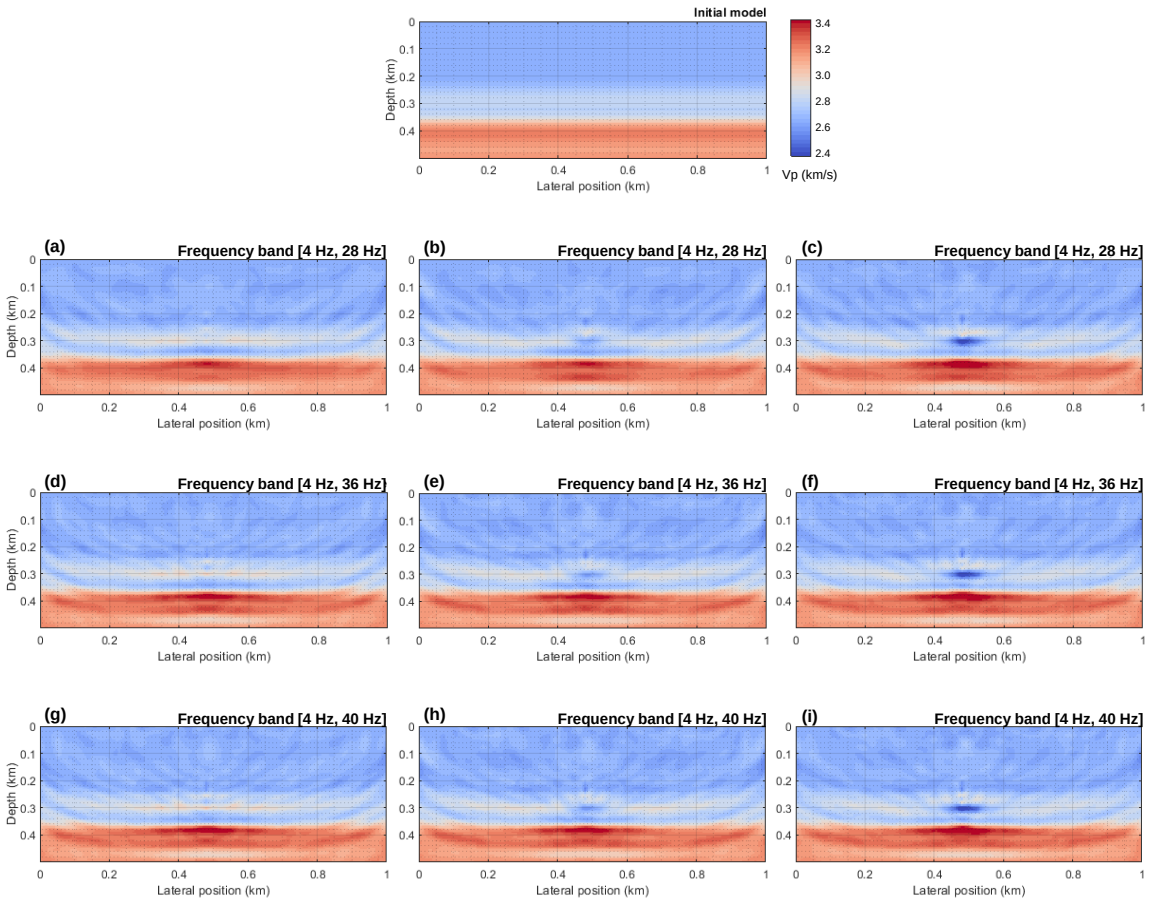

FIG. 8. Inverted models utilizing the permanent VSP experiment design with sensors deployed between 190 to 305 m and a source distribution spaced every 142 m for three different frequency bands at three different stages. Graphs (a), (d) and (g) represent the inverted baseline models, whereas (b), (e) and (h) represent the inverted models after one year of CO_2 injection; and (c), (f) and (i) represent the inverted models after five years of CO_2 injection.

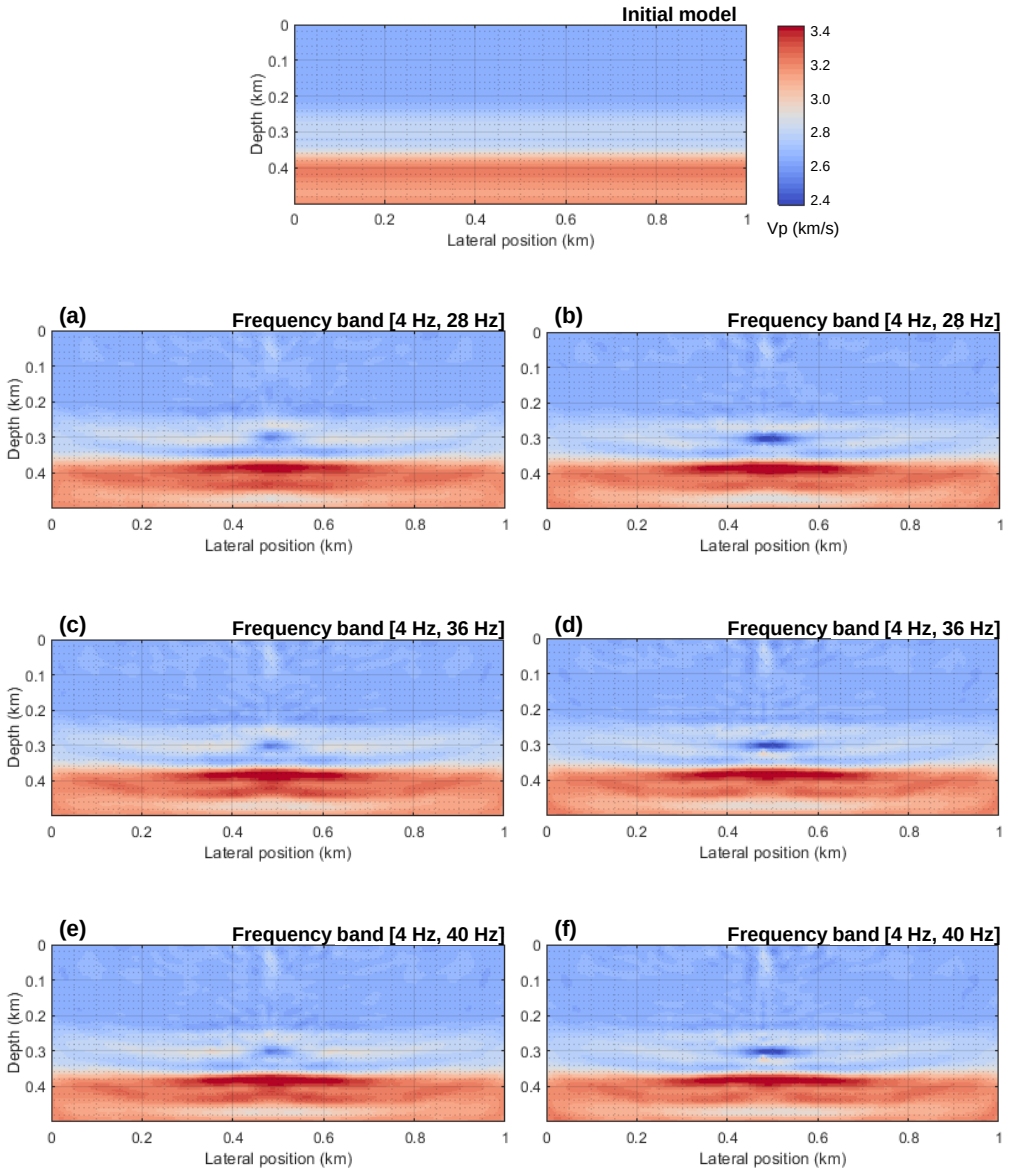

FIG. 9. Inverted models utilizing the 2018 VSP experiment design with sensors deployed between 0 to 324 m and a source distribution spaced every 142 m for three different frequency bands at three different stages. Graphs (a), (c) and (e) correspond to the inverted models after one year of CO_2 injection, while (b), (d) and (f) correspond to the inverted models after five years of CO_2 injection.

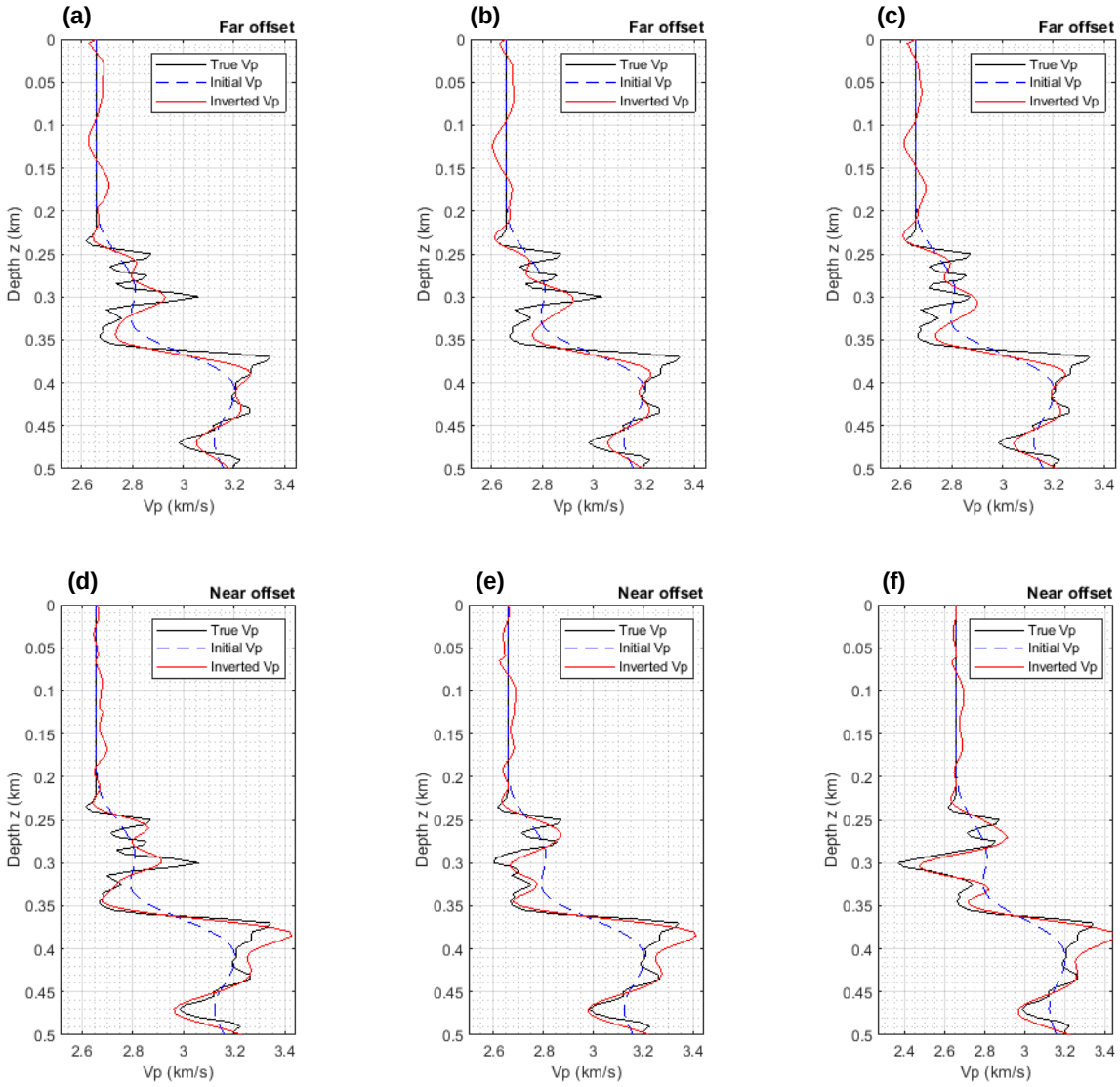

FIG. 10. Profile views of the true, initial and inverted P-wave velocity for far and near offsets modeling the permanent sensors disposition set at the FRS with fewer sources, for three different stages. Graphs (a) and (d) represent the baseline stage, while (b) and (e) represent the effects of one year of CO_2 injection; and (c) and (d) represent the effects of five years of CO_2 injection.

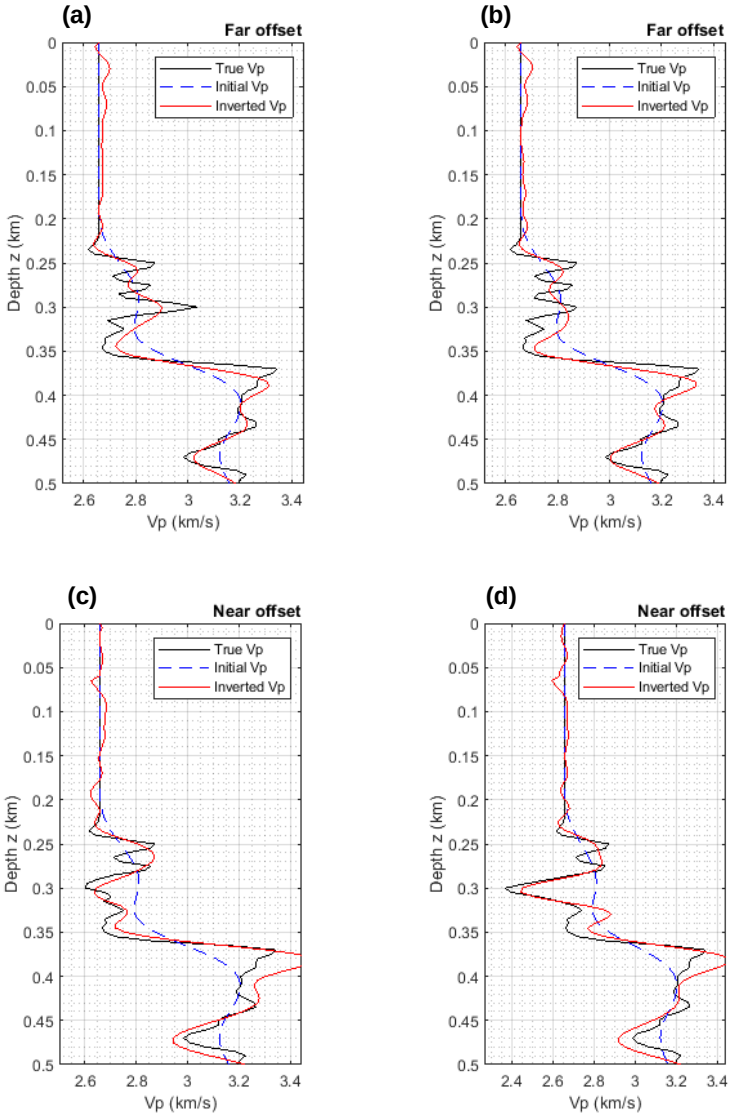

FIG. 11. Profile views of the true, initial and inverted P-wave velocity for far and near offsets modeling the 2018 sensors disposition at the FRS with fewer sources for three different stages. Graphs (a) and (c) represent the effects of one year of CO_2 injection; while (b) and (d) represent the effects of five years of CO_2 injection.

Figure 12 illustrates a profile comparison of the inverted P-wave velocity at near and far offsets for the three modeled stages, providing us with a time-lapse estimation for the FRS based entirely on FWI. The four top panels correspond to the computed results using the permanent sensor distribution, while bottom panels present the inverted values utilizing the 2018 VSP receiver disposition. Diagrams in columns (a), (b), (e) and (f) were modeled with a source spacing of 60 m, whereas for columns (c), (d), (g) and (h), the source spacing was 142 m.

The baseline model was only inverted using the permanent receiver arrangement to keep consistency with the existing real data from the FRS. Hence, all comparisons labeled as baseline Vp in the time-lapse graphs correspond to this particular configuration, including for results modeled using the 2018 receiver disposition.

DISCUSSION

Inversion results demonstrate the potential of FWI to record and monitor changes in the reservoir levels at CaMI FRS for the compressional wave velocity. Model resolution does not appear to be particularly influenced by the amount and distribution of receivers at this geological setting, as much as it is controlled by number of modeled sources. The latter have profound impact in the amount of seismic rays that sample the medium, and therefore, how it is illuminated, the resolvable features in it and shape of the inverted models, which for this study exhibit the cone-shape fashion associated with VSP.

Figure 4 follows the time evolution of the effects of CO_2 from a baseline to a five-year period using the permanent experiment. In general terms, we observed a refinement of model features once we reach medium band frequencies for intervals above and below the reservoir level, which helps to constraint the vertical expansion of the P-wave velocity reduction zone. The limits of the lateral variations produced by the gas injection are harder to visualize than the vertical ones because they are associated with lateral resolution of the seismic experiment. Hence, velocity changes for near offsets are modeled with higher precision and tend to converge towards the true values at all depths if compared with estimations made for far offsets. This is more evident in profile views of the same final medium frequency band of [4 Hz, 40 Hz] inverted model, as Figure 6 displays.

Results obtained using the 2018 VSP sensors arrangement and an equal source distribution set for the permanent experiment of about 60 m, do not seem to provide further enhancement at the reservoir interval, as Figures 5 and 7 illustrate. However, they emphasize slightly better the edges CO_2 effects in the inverted velocity values, especially for the projections made after one-year injection. All inverted models with this configuration present shallow velocity artifacts centered on the well that are associated with sources and the ray paths recorded at upper receivers which do not have much detail to invert for.

As Figure 8 shows, reduction in the number sources decreases significantly the ability to distinguish velocity variations in the model because illumination becomes more limited. Even ray paths can appear in the inverted models like oblique patterns at all depth levels, leading us to notice which areas were actually sampled and updated in the inversion process. This imaging impoverishment can be trace into the frequency spectrum content of the dataset, therefore it is entirety associated with each survey and it is not related with the multiscale approach utilized. Though, for this test we employed an equivalent FWI scheme as for previous cases, including a similar number of maximum iterations per band and migrated frequencies, the inverted models still look very smooth in various areas. In fact, the profiles views of this inversion displayed in Figure 10 suggest that at near offsets the inverted velocity somehow converged towards the true solution, but as lateral distance increases the inversion resembles our initial model.

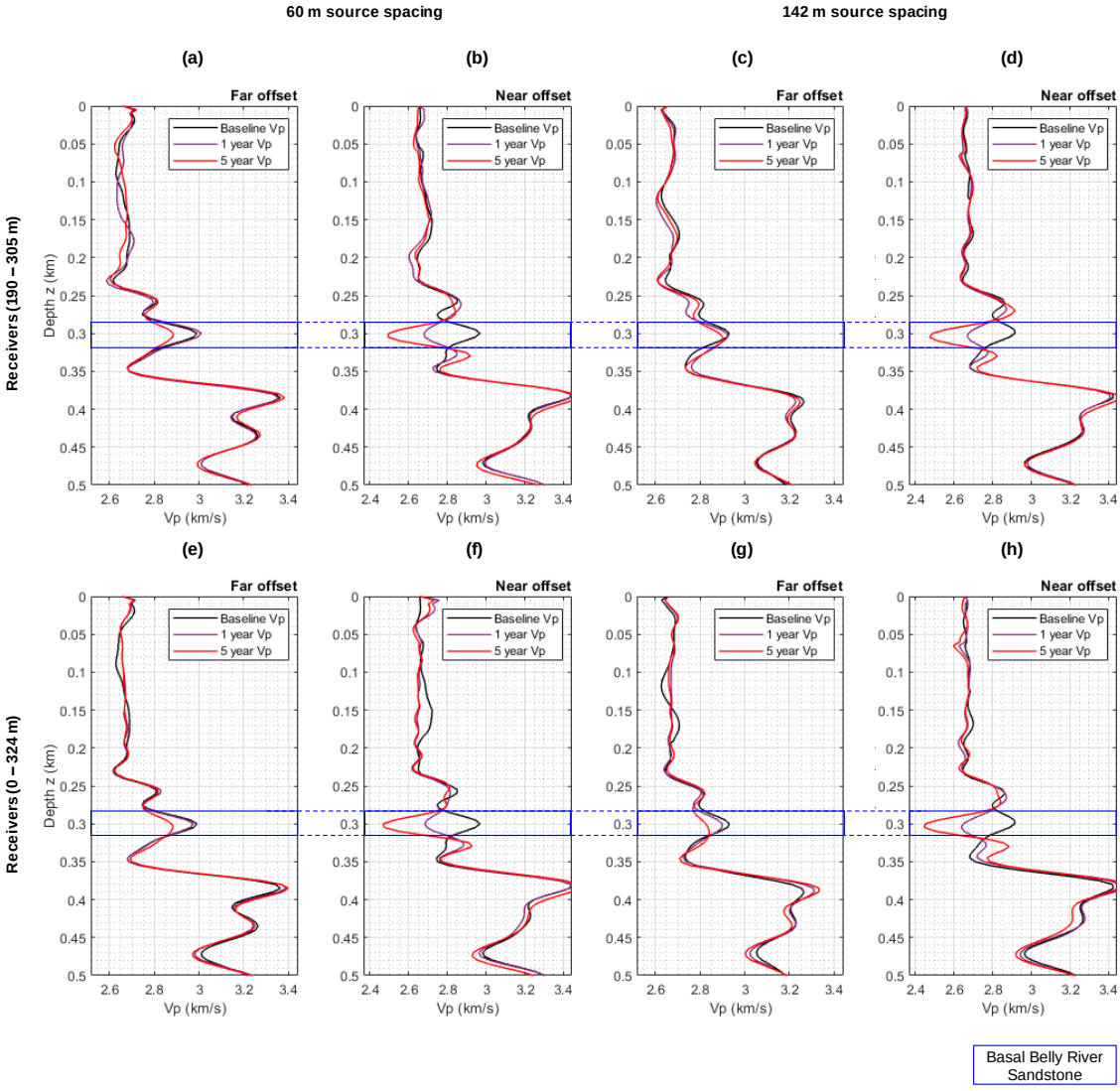

FIG. 12. Time-lapse evolution of the inverted velocity for the three modeled stages of CO_2 injection at depth levels around the Basal Belly River Sandstone. Near and far offsets views were obtained modeling the permanent receiver arrangement between 190 to 305 m in (a) and (b) with a source distribution spaced every 60 m; and in (c) and (d) with a source distribution spaced every 142 m. Whereas, the others near and far offsets views were obtained modeling the 2018 receiver arrangement between 0 to 324 m in (e) and (f) with a source distribution spaced every 60 m; and in (g) and (h) with a source distribution spaced every 142 m.

A similar behaviour was observed when we modeled the 2018 sensor distribution with fewer sources, as Figures 9 and 11 demonstrate. Although in this case, it proved to be beneficial having a dense receiver distribution to image the velocity variations, if it is compared with inversion results using the permanent sensor configuration. Inverted models for the fifth year of CO_2 injection failed to capture the lateral boundaries of the P-wave velocity changes.

Figure 12 displays the inverted P-wave velocity from all tested models during this investigation at near and far offset locations, giving us a time-lapse view of the FRS

utilizing an acoustic FWI algorithm. The interval of around the BBRS is highlighted in all diagrams and it emphasizes a reduction in the velocity in all cases, even for the experiments with sparse modeled sources. As it has been discussed, comparable results were obtained for inverted models with the same source distribution, despite the number and depth levels of the sensors used to the modeled VSP. This is ultimately a positive aspect because the permanent experiment deployed at the FRS has a limited range of receivers.

Lastly, we only registered a maximum 17% of velocity decrease at the reservoir level in our best case scenario, which entails a source distribution of about 60 m. Although, this number falls behind the projections made for this site, we can attribute it to a lower and limited seismic resolution. Yet, results encourage us to procced inverting for the elastic rock parameters at CaMI FRS and utilize this methodology as a time-lapse tool to monitor the effects of a carbon dioxide injection.

ACKNOWLEDGEMENTS

The authors thank the sponsors of CREWES for continued support. This work was funded by CREWES industrial sponsors, and NSERC (Natural Science and Engineering Research Council of Canada) through the grants CRDPJ 461179-13. The acoustic FWI code utilized in this investigation was adapted from S. Romahn thesis, for which he is gratefully acknowledged.

REFERENCES

Amundaray, N., and Innanen, K. A. H., 2020, Time domain FWI in MatLab with applications to inversion of simulated VSP data: CREWES Research Report, **32**, 1.

Cova, R., Innanen, K. A. H., and Rauch-Davies, M., 2018, Walkaway VSP data conditioning for FWI: CREWES Research Report, **30**, 08.

Hall, K. W., Bertram, K. L., Bertram, M., Innanen, K. A. H., and Lawton, D. C., 2018, CREWES 2018 multi-azimuth walk-away VSP field experiment: CREWES Research Report, **30**, 16.

Hamblin, A. P., and Abrahamson, B. W. (1996). Stratigraphic architecture of "Basal Belly River" cycles, Foremost Formation, Belly River Group, subsurface of southern Alberta and southwestern Saskatchewan: Bulletin of Canadian Petroleum Geology, **44**, 654–673.

Lumley, D. E., 2001, Time-lapse seismic reservoir monitoring: Geophysics, 66, 50–53.

Macquet, M., Lawton, D., Saeefdar, A., and Osadetz, K., 2019, A feasibility study for detection for detections thresholds of CO2 at shallow depths at the CaMI Field Research Station, Newell County, Alberta, Canada: Petroleum Geoscience, No. 25(4):509.

Pan, W., Innanen, K. A., and Geng, Y., 2018, Elastic full-waveform inversion and parametrization analysis applied to walk-away vertical seismic profile data for unconventional (heavy oil) reservoir characterization: Geophysical Journal International, **213**, 1934–1968.

Smithyman, B.R, Peters, B., and Herrmann, F.J., 2015, Constrained Waveform Inversion of Colocated VSP and Surface Seismic Data: 77th EAGE Conference and Exhibition.

Wright, G.N., McMechan, M.E., Potter, D.E.G. and Holter, M.E. 1994. Structure and architecture of theWestern Canada Sedimentary Basin. In: Mossop, G.D. & Shetsen, I.(eds) Geological Atlas of the Western Canada Sedimentary Basin. Canadian Society of Petroleum Geologists and Alberta Research Council, Calgary, 25–40.